

Ni-impurity effects on the superconducting gap of $\text{La}_{2-x}\text{Sr}_x\text{CuO}_4$ studied from the magnetic field and temperature dependence of the electronic specific heat

T. Kurosawa,¹ N. Momono,² M. Oda,¹ and M. Ido¹

¹*Department of Physics, Hokkaido University, Sapporo 060-0810, Japan*

²*Department of Applied Sciences, Muroran Institute of Technology, Muroran 050-8585, Japan*

(Dated: November 7, 2018)

The magnetic field and temperature dependence of the electronic specific heat C_{el} have been systematically investigated in $\text{La}_{2-x}\text{Sr}_x\text{Cu}_{1-y}\text{Ni}_y\text{O}_4$ (LSCNO) in order to study Ni-impurity effects on the superconducting (SC) gap. In LSCNO with $x=0.15$ and $y=0.015$, the value of γ ($\equiv C_{\text{el}}/T$) at $T=0$ K, γ_0 , is enhanced under the magnetic field H applied along the c -axis. The increment of γ_0 , $\Delta\gamma_0$, follows the Volovik relation $\Delta\gamma_0=A\sqrt{H}$, characteristic of the SC gap with line nodes, with prefactor A similar to that of a pure sample. The C_{el}/T vs. T curve under $H=0$ shows a d -wave-like SC anomaly with an abrupt increase at T_c and T -linear dependence at $T\ll T_c$, although the γ_0 -value in the C_{el}/T vs. T curve increases with increasing Ni concentrations. Interestingly, as the SC part of C_{el}/T , $C_{\text{el}}/T-\gamma_0\equiv\gamma_s$, decreases in LSCNO, T_c is reduced in proportion to the decrease of γ_s . These findings can be explained phenomenologically by a simple model in which Ni impurities bring about strong pair breaking at the edges of the coherent nodal part of the Fermi surface but in the vicinity of the nodes of the SC gap. The reduction of the SC condensation energy U_0 in LSCNO, evaluated from C_{el} at $T\lesssim T_c$, is also understood by the same model.

PACS numbers: 74.62.En, 74.72.-h,

I. INTRODUCTION

One of the striking features in high- T_c cuprates is an unusual impurity effect on the superconductivity, which has been studied extensively from experimental and theoretical points of view to elucidate the mechanism for high- T_c superconductivity. As is well known, in conventional superconductors, whose superconducting (SC) order parameter is of the s -wave type, magnetic impurities strongly suppress T_c ¹, whereas nonmagnetic ones do little². However, this is not the case for the impurity effect on high- T_c superconductivity, whose order parameter is of the d -wave type. In high- T_c cuprates, a small number of in-plane impurities, such as nonmagnetic Zn or magnetic Ni impurities, which are partially substituted for Cu sites within CuO_2 planes, cause a large reduction of T_c and a large increase of the residual density of states (DOS) at the Fermi level (E_F), whether they are magnetic or not.³⁻⁸ More interestingly, it has been demonstrated in $\text{La}_{2-x}\text{Sr}_x\text{CuO}_4$ (LSCO) that a nonmagnetic Zn impurity exhibits a stronger effect on the high- T_c superconductivity than a magnetic Ni impurity; in particular, the recovery of the residual DOS(E_F) is much more evident for the former impurity.⁶⁻⁸ The large recovery of the residual DOS(E_F) due to a small amount of Zn impurity has been explained well in terms of a model in which the SC gap is completely suppressed locally in areas with a diameter on the order of the antiferromagnetic (AF) correlation length around the Zn impurity, where the AF correlation among Cu spins is disturbed because there are no localized spins on the impurity sites.^{7,9} However, such a model gives no explanation for the large suppression of T_c in the SC region outside the magnetically disturbed areas around Zn impurities. Furthermore, the mechanism for the suppression of superconductivity in

Ni-doped LSCO has not been clarified yet. It has been demonstrated in measurements of the T dependence of magnetic susceptibility in pure and Ni-doped LSCO that a small amount of Ni impurity, which has a localized spin, has little effect on the AF correlation among Cu-spins, as in the SC region outside the non-SC areas around Zn impurities.^{7,10} Therefore, the suppression of superconductivity in Ni-doped LSCO is expected to occur rather uniformly over the whole crystal, which is much simpler than that in Zn-doped LSCO.

In d -wave superconductors, it has been broadly thought that the presence of impurities gives rise to pair breaking in the vicinity of the nodes and leads to collapse of the SC gap there.¹¹ However, in our recent study on the low-temperature ($T\ll T_c$) electronic specific heat of Ni-doped LSCO, we pointed out that the SC gap around the nodes will be affected only slightly by a small amount of Ni impurity.¹² Furthermore, recent angle-resolved photoemission spectroscopy (ARPES) experiments on $\text{Bi}_2\text{Sr}_{2-x}\text{R}_x\text{CuO}_{6+\delta}$ (R -Bi2201, R : rare earth element) reported that as interplane disorders, which are caused by the substitution of R atoms for Sr sites, are strengthened by replacing the R atom La with Eu, the T_c is reduced from 33 K to 18 K at the optimal doping level, but the SC gap dispersion around the nodes remains almost unchanged. The suppression of superconductivity in Eu-Bi2201 has been discussed in terms of the shrinkage of a nodal part of the Fermi surface (FS), the so-called “Fermi arc”, which consists of coherent electronic states and is responsible for an effective SC gap in determining T_c .¹³ On the other hand, it has been claimed in ARPES experiments on $\text{Bi}_2\text{Sr}_2\text{CaCu}_{2-x}\text{M}_x\text{O}_{8+\delta}$ (M -Bi2212, M =Ni or Zn) that the SC gap is collapsed in the vicinity of the nodes. However, its region around the nodes is only $\sim 2\%$ of the whole FS, corresponding to the

region whose original gap size is smaller than ~ 1 meV, which would be too small to explain the observed reduction of T_c ($\Delta T_c=5-10$ K).¹⁴ Thus, in high- T_c cuprates, the impurity or disorder effect on the SC gap is still under debate even for the nodal region.

One of the good ways to investigate the SC gap around the nodes in d -wave superconductors is to measure the electronic specific heat C_{el} in the SC mixed state induced by the application of magnetic field H along the lines of nodes. In the mixed state, the electronic specific heat coefficient γ ($\equiv C_{el}/T$) at $T=0$ K, the residual γ value, γ_0 , reflecting the residual DOS(E_F), increases with the increase of H . This is because the residual DOS(E_F) recovers in areas extending along the node directions from vortex cores, which is due to the Doppler shift of the quasiparticle dispersion curve. The increment of γ_0 , $\Delta\gamma_0$, follows the Volovik relation, $\Delta\gamma_0=A\sqrt{H}$, where prefactor A is inversely proportional to the slope v_Δ of the gap dispersion around the nodes.¹⁵ The Volovik relation has been confirmed in pure samples of $\text{YBa}_2\text{Cu}_3\text{O}_7$ ¹⁶ and LSCO ^{17,18}.

In the present study, the Ni-impurity effect on the SC gap was examined from measurements of the electronic specific heat C_{el} at $T \ll T_c$ under magnetic fields for $\text{La}_{2-x}\text{Sr}_x\text{Cu}_{1-y}\text{Ni}_y\text{O}_4$ (LSCNO) samples. First, we report that the residual γ value ($\equiv C_{el}/T$) at $T=0$ K, γ_0 , increases under magnetic fields, following the Volovik relation, in LSCNO as well as in pure samples. Next we report that the SC part of C_{el}/T , $C_{el}(T, y)/T - \gamma_0(y) \equiv \gamma_s(T, y)$, under $H=0$ shows a SC anomaly exhibiting an abrupt increase at T_c and T -linear dependence at $T \ll T_c$, although the SC anomaly is largely suppressed as a whole with increases in Ni-concentration y . Furthermore, T_c is reduced in proportion to the suppression of $\gamma_s(T, y)$ in LSCNO. On the basis of these observations, we propose a scenario in which the SC gap of LSCNO will be predominantly suppressed not in the vicinity of the nodes but at the edges of the coherent nodal FS. Such Ni-impurity pair breaking leads to natural explanations for the marked suppression of T_c and the SC condensation energy U_0 , evaluated from the data of $\gamma_s(T, y)$, in LSCNO.

II. EXPERIMENTAL PROCEDURES

Specific heat measurements at low temperatures ($T < 10$ K) under magnetic fields, whose directions were perpendicular to CuO_2 planes, that is, along the c -axis, were carried out by a thermal relaxation method in single crystal samples of LSCNO. On the other hand, specific heat measurements in a wide T range from 4 K to 60 K, sufficiently higher than T_c , under a zero magnetic field were carried out by a conventional heat-pulse technique on ceramic samples of LSCNO. The way to determine the T dependence of the phonon term $C_{ph}(T)$ in a wide T range is one of the important keys to extracting the change of $C_{el}(T)$ in accordance with the SC transition

from the total specific heat $C(T)$, including both the $C_{el}(T)$ and $C_{ph}(T)$ terms. The partial Ni substitution for Cu sites makes it possible to determine the phonon term $C_{ph}(T)$ of the SC samples. This is because a small amount of Ni substitution can destroy the superconductivity completely but has little effect on the phonon term, at least, in the optimal samples.⁷ This Ni substitution effect is in sharp contrast with Zn substitution, which modifies the phonon term significantly. In the present study, we obtained the electronic term $C_{el}(T)$ by subtracting the phonon term $C_{ph}^{\text{Ni}}(T)$, which was estimated in a Ni-doped non-SC sample, from the observed, total specific heat $C(T)$; $C_{el}(T) = C(T) - C_{ph}^{\text{Ni}}(T)$. Details of the estimations of $C_{ph}^{\text{Ni}}(T)$ and/or $C_{el}(T)$ have been published elsewhere.¹⁹⁻²¹

Ceramic and single-crystal samples of LSCNO were prepared by using La_2O_3 , SrCO_3 , CuO , and NiO powders of 99.99-99.999% purity. For the ceramic samples, these powders were mixed well and then heat-treated in a furnace at a certain temperature under flowing oxygen. The heat-treated materials were reground well and pressed into pellets, and were sintered in flowing oxygen. The single crystal samples were grown by the traveling solvent floating zone method. For these ceramic and single crystal samples, the SC critical temperature T_c was determined from the SC diamagnetism measured with a SQUID magnetometer.

III. RESULTS AND DISCUSSION

A. Electronic specific Heat in the Mixed State of $\text{La}_{2-x}\text{Sr}_x\text{Cu}_{1-y}\text{Ni}_y\text{O}_4$

In $\text{La}_{2-x}\text{Sr}_x\text{Cu}_{1-y}\text{Ni}_y\text{O}_4$ (LSCNO) with $x=0.15$, the C/T vs. T^2 curve at $H=0$ follows a straight line at $T \ll T_c$, because the electronic T^2 term arising from low-energy quasiparticle excitations around the line nodes at $T \ll T_c$ is much smaller than the phonon T^3 term except the nearly over-doped region.^{22,23} Applying a magnetic field to the pure crystal with $y=0$ along the direction perpendicular to the CuO_2 plane (the c -axis), the C/T vs. T^2 curve shifts upward as a whole, indicating that the value of γ_0 is enhanced under magnetic fields through the Doppler shift of the quasiparticle dispersion curve, as shown in Fig. 1(a) in ref. (12). In the present study, we obtained the H dependence of γ_0 , $\gamma_0(H)$, up to 10 T more precisely than in our previous work (Fig. 1). One can see that the increment of γ_0 , $\Delta\gamma_0 [\equiv \gamma_0(H) - \gamma_0(0)]$, follows the Volovik relation $\Delta\gamma_0 = A\sqrt{H}$, as has been reported for pure high- T_c cuprates¹⁶⁻¹⁸.

Prefactor A in the Volovik relation is written as²⁴

$$A = \frac{4k_B^2}{3\hbar} \sqrt{\frac{\pi}{\Phi_0}} \frac{nV_{\text{mol}}}{l_c} \frac{\eta}{v_\Delta}. \quad (1)$$

In this expression, v_Δ is the slope of the d -wave gap dispersion around the nodes, n the number of CuO_2 planes

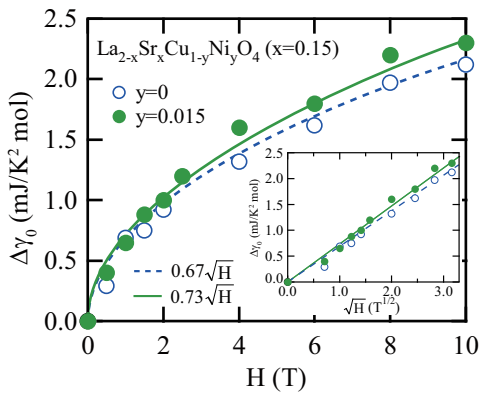


FIG. 1: (Color online) Magnetic field dependence of $\Delta\gamma_0 = \gamma_0(H) - \gamma_0(0)$ in pure $\text{La}_{2-x}\text{Sr}_x\text{CuO}_4$ ($x=0.15$, $T_c=37.0$ K) (open circles) and that of $\text{La}_{2-x}\text{Sr}_x\text{Cu}_{1-y}\text{Ni}_y\text{O}_4$ ($x=0.15$, $y=0.015$, $T_c=26.5$ K) (closed circles) samples. The solid and dashed lines represent functions of \sqrt{H} . The inset shows $\Delta\gamma_0$ vs. \sqrt{H} plots.

within the unit cell, l_c the lattice constant along the c -axis, and V_{mol} the volume of a mole. Prefactor A also depends on the parameter η ; η is $\eta=0.5$ for a square flux-line lattice and $\eta=0.47$ for a triangular one. Small angle neutron scattering experiments on nearly optimally doped and overdoped LSCO crystals under magnetic fields parallel to the c -axis have demonstrated that the vortex lattice is of a triangular type for low fields and gradually changes into a square type around $H \sim 0.5$ T.²⁵ The magnetic fields ($0.5 \text{ T} \leq H \leq 10 \text{ T}$) used in the present study on LSCNO with $x=0.15$ were in the H range of the square-type lattice. Thus, using the experimental value of A and $\eta=0.5$, v_Δ is estimated to be 6.1×10^5 cm/s from Eq. 1. This value for v_Δ is in good agreement with that obtained in ARPES experiments on LSCO crystals with $x \sim 0.15$.^{26–28}

The H dependence of C/T vs. T^2 curves for LSCNO with $x=0.15$ and $y=0.015$, whose T_c ($=26.5$ K) is $\sim 30\%$ lower than that of the pure crystal is shown in Fig. 1(b) in ref. (12). One can see in this figure that the C/T vs. T^2 curve also shifts upward as a whole under magnetic fields; that is, the value of γ_0 is enhanced in the LSCNO sample by the Doppler shift of the quasiparticle dispersion curve. We estimate the γ_0 value under magnetic fields from C/T vs. T^2 curves of LSCNO in the same way as in the pure crystal, and plot the increment of γ_0 , $\Delta\gamma_0 [= \gamma_0(H) - \gamma_0(0)]$, as a function of H in Fig. 1. The $\Delta\gamma_0$ thus estimated also satisfies the Volovik relation $\Delta\gamma_0 = A\sqrt{H}$, although prefactor A in the present LSCNO is slightly larger than that in the pure crystal. The maintenance of the Volovik relation means that nodes remain in the SC gap in LSCNO as if they are almost free from the pair breaking with Ni impurity. According to Eq. 1, the present increment of A leads to a 9% reduction of v_Δ . Since v_Δ is proportional to the gap maximum Δ_0 (see Eq. 1), T_c is expected to decrease in accordance with

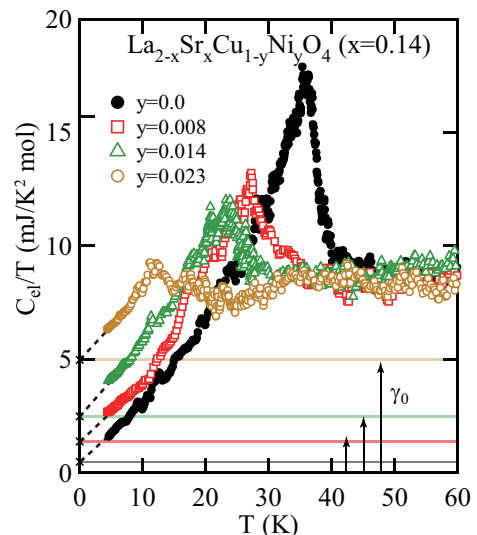


FIG. 2: (Color online) $C_{\text{el}}(T)/T$ vs. T plots for $\text{La}_{2-x}\text{Sr}_x\text{Cu}_{1-y}\text{Ni}_y\text{O}_4$ with $x=0.14$. The Ni concentration y and the corresponding T_c are as follows: $y=0$ ($T_c=36.8$ K), $y=0.008$ ($T_c=28.8$ K), $y=0.014$ ($T_c=24.3$ K), and $y=0.023$ ($T_c=13.0$ K).

the reduction of v_Δ . However, in the present experimental result, the 9% reduction of v_Δ is too small to explain the $\sim 30\%$ reduction of T_c .

B. Temperature dependence of the electronic specific heat C_{el} in $\text{La}_{2-x}\text{Sr}_x\text{Cu}_{1-y}\text{Ni}_y\text{O}_4$

Figure 2 shows the electronic specific heat $C_{\text{el}}(T)/T$ over a wide T range from 4 K to 60 K for slightly underdoped LSCNO ceramics ($x=0.14$, $y=0, 0.008, 0.014$, and 0.023). In the pure sample ($y=0$), the $C_{\text{el}}(T)/T$ vs. T curve with a very small γ_0 exhibits a SC anomaly with an abrupt increase around T_c and a T -linear dependence at $T \ll T_c$. The T -linear dependence at $T \ll T_c$ originates in the existence of the line nodes in the SC gap. In LSCNO samples, the γ_0 value in the $C_{\text{el}}(T)/T$ vs. T curve is largely enhanced, meaning that parts of the FS revive on account of pair breaking caused by Ni impurity (Fig. 2). As γ_0 is enhanced with the increase of the Ni-impurity concentration y , the SC anomaly shifts toward low temperatures as a whole, and is suppressed with the increase of y , as seen in Fig. 2.

Here we pay attention to the SC part of $C_{\text{el}}(T, y)/T$, namely, $C_{\text{el}}(T, y)/T - \gamma_0(y)$. We normalize the SC part $C_{\text{el}}(T, y)/T - \gamma_0(y) \equiv \gamma_s(T, y)$ with its normal state value $\gamma_n(y) - \gamma_0(y)$, and plot it as a function of $T/T_c(y)$ in Fig. 3(a) for $x=0.14$ and 3(b) for $x=0.16$. The normalized SC parts are in agreement with each other, including that of the pure sample, though the jump at T_c is smeared in some degree in LSCNO, as seen in Fig. 3. Such agreement indicates that $\gamma_n(y) - \gamma_0(y)$ reflects the frac-

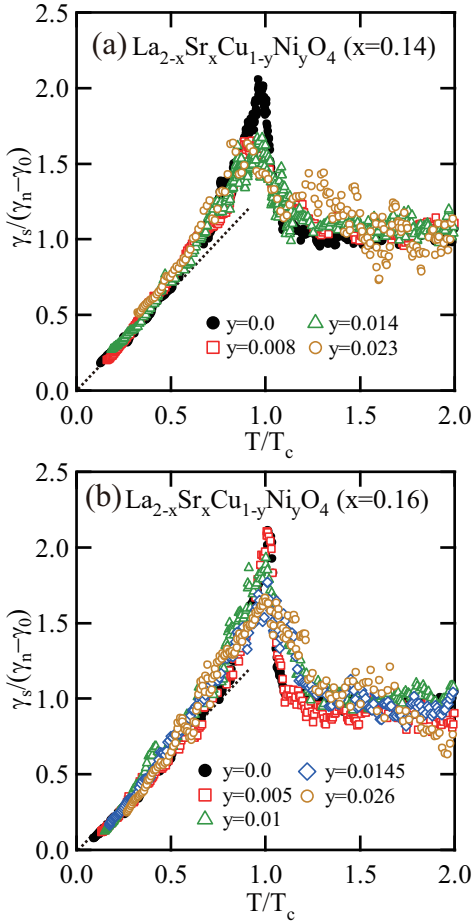


FIG. 3: (Color online) $\gamma_s/(\gamma_n-\gamma_0)$ vs. T/T_c plots for $\text{La}_{2-x}\text{Sr}_x\text{Cu}_{1-y}\text{Ni}_y\text{O}_4$ samples with (a) $x=0.14$ and (b) $x=0.16$.

tion of the quasiparticles which become SC condensates at $T \ll T_c$. Actually, $\gamma_n(y) - \gamma_0(y)$, which largely decreases with increasing y , closely relates to the rapid suppression of $T_c(y)$ in LSCNO, as shown in Fig. 4. The close relation between $\gamma_n(y) - \gamma_0(y)$ and $T_c(y)$ is expected to provide a key to understanding the Ni-impurity effect. It is also worth noting that the normalized $\gamma_s(T, y)$ vs. T plot shows the T -linear dependence at $T \ll T_c(y)$ in all samples, including the pure sample, as seen in Fig. 3. This result implies that the line nodes remain in the SC gap of LSCNO, which is consistent with the present findings in specific heat measurements under magnetic fields.

On the basis of the above results and discussion, we propose the following simple scenario for the Ni-impurity effect on the SC gap. The SC gap is suppressed predominantly on segments of the FS away from the nodes, but remains virtually unchanged in the vicinity of the nodes. The former segments of the FS, where the SC gap is predominantly suppressed, lead to the T -independent part $\gamma_0(y)$ in the $C_{el}(T, y)/T$ vs. T curve through the revival of the DOS(E_F) resulting from the local suppression of

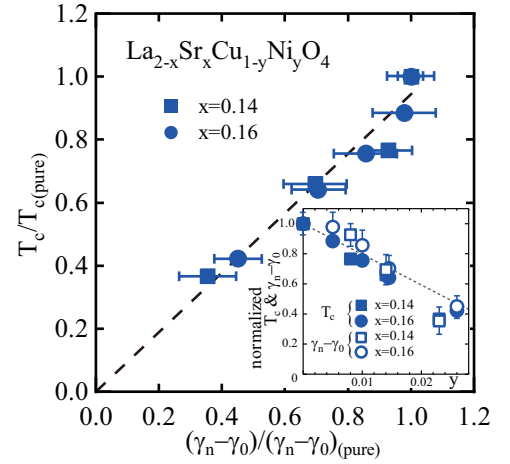


FIG. 4: (Color online) $T_c/T_{c(\text{pure})}$ vs. $(\gamma_n-\gamma_0)/(\gamma_n-\gamma_0)_{(\text{pure})}$ plots for $\text{La}_{2-x}\text{Sr}_x\text{Cu}_{1-y}\text{Ni}_y\text{O}_4$ with $x=0.14$ and $x=0.16$. The inset shows the y dependence of T_c and $\gamma_n-\gamma_0$ value normalized with those of the pure sample, $T_{c(\text{pure})}$ and $(\gamma_n-\gamma_0)_{(\text{pure})}$, respectively.

the SC gap. On the other hand, the latter nodal segments are SC segments and responsible for the SC part $\gamma_s(T, y)$. In such a case, the length $L(y)$ of the SC nodal segment is proportional to $\gamma_n(y) - \gamma_0(y)$; $L(y) \propto \gamma_n(y) - \gamma_0(y)$. On the basis of the relation $L(y) \propto \gamma_n(y) - \gamma_0(y)$ and the coherent SC nodal segment (the Fermi arc), we will discuss the marked suppression of T_c and the SC condensation energy U_0 in detail within the present scenario in subsection III D.

C. Superconducting condensation energy of $\text{La}_{2-x}\text{Sr}_x\text{Cu}_{1-y}\text{Ni}_y\text{O}_4$

In this subsection, we discuss the SC condensation energy U_0 of LSCNO, which was evaluated from the present data of $\gamma_s(T, y)$. The condensation energy U_0 at $T=0$ K is given by integrating the entropy difference $S_n - S_s$ from $T=0$ K to the temperature T_{sf} , around which the SC anomaly starts to evolve, slightly higher than T_c ,

$$U_0 = \int_0^{T_{\text{sf}}} (S_n - S_s) dT, \quad (2)$$

the subscripts “s” and “n” stand for the SC and hypothetical normal states at $T < T_{\text{sf}}$, respectively. Given both $\gamma_s(T)$ and $\gamma_n(T)$ as functions of T , we can obtain the entropy $S_s(T)$ and $S_n(T)$ by executing the integration

$$S_{s,n}(T) = \int_0^T \gamma_{s,n}(T) dT, \quad (3)$$

and evaluate the condensation energy U_0 using Eq. 2.²⁹ In this study, $\gamma_n(T)$ was obtained by linear extrapolation of high-temperature data in the normal state down to

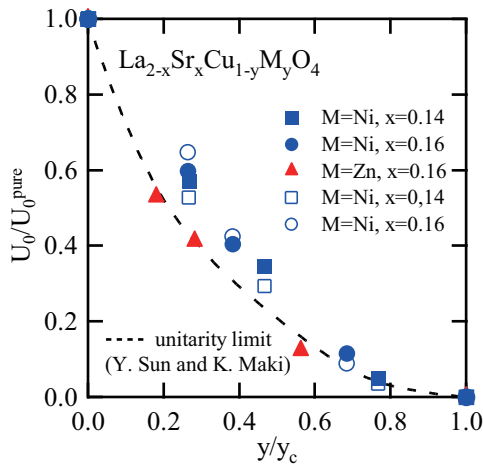


FIG. 5: (Color online) The SC condensation energy U_0 for $\text{La}_{2-x}\text{Sr}_x\text{Cu}_{1-y}\text{Ni}_y\text{O}_4$ for $x=0.14$ and $x=0.16$ and $\text{La}_{2-x}\text{Sr}_x\text{Cu}_{1-y}\text{Zn}_y\text{O}_4$ for $x=0.16$. Closed symbols are the values obtained from the $C_{\text{el}}(T)/T$ vs. T curve, and open symbols are the values calculated by modifying the BCS formula for U_0 (Eq. 4). The dashed line represents the result numerically calculated in the unitarity limit by Sun and Maki.³⁰

below T_c so as to satisfy the so-called “entropy balance”; namely, the constraint that both $S_s(T)$ and $S_n(T)$ values must be equal to each other at T_{sf} .^{20,21}

The SC condensation energy U_0 thus evaluated is plotted as a function of the Ni-concentration y in Fig. 5, where U_0 and y are normalized with U_0 of the pure sample, U_0^{pure} , and y_c at which the superconductivity is completely suppressed. In Fig. 5, U_0 of samples doped with nonmagnetic Zn impurities, evaluated as in the case of Ni impurity, is also shown for comparison. The broken line in this figure represents the theoretical result calculated by Sun and Maki for d -wave superconductors with impurities (pair-breaking centers) in the unitarity limit, which suppress the SC gap (the SC order parameter) completely at impurity sites.³⁰ In Zn-doped samples whose SC gap is completely suppressed around the impurities, the experimental values of U_0 just fall upon the broken line predicted by the Sun and Maki theory in the unitarity limit (Fig. 5), as expected. On the other hand, in Ni-doped samples, the experimental result deviates upward from the theoretical curve, as seen in Fig. 5. This fact suggests that Ni impurities will not be in the unitarity limit, and that the suppression of superconductivity will occur predominantly not only around the impurities but uniformly over the whole crystal.^{6,7}

D. Effective SC gap in $\text{La}_{2-x}\text{Sr}_x\text{Cu}_{1-y}\text{Ni}_y\text{O}_4$

In d -wave superconductors, it has been broadly thought that impurities will cause pair breaking predominantly in the vicinity of the nodes where the excitation energies of quasiparticles are very small, and that the

SC gap would collapse around the nodes. Indeed, in the case of strong impurities in the unitarity limit, whose potential is isotropic and given by the δ -function, Sun and Maki demonstrated that the SC gap will collapse on the FS around the node.³⁰ Furthermore, when the potential of strong impurities is anisotropic or momentum dependent, it was predicted by Haas *et al.* that the SC gap would also be strongly suppressed around the nodes rather than around the antinodes on the FS.¹¹ However, such a result seems to be incompatible with the experimental finding that definite nodes remain in the SC gap in LSCNO. On the other hand, Toyama and Ohkawa have discussed the effect of a small number of weak impurities on d -wave superconductors on the basis of a self-consistent Born approximation, and shown that the SC gap will be little affected around the nodes as in the present case, whereas it will rather be suppressed around the antinodes through strong scattering of quasiparticles.³¹ However, it seems difficult for this model to reproduce a large recovery of the residual γ , $\gamma_0(y)$, caused by a small amount of Ni impurity as observed in LSCNO, although the model explains a large reduction of T_c well.

In high- T_c cuprates, it has been demonstrated that the FS is divided into two segments with different characters. One of them comprises coherent nodal segments of the FS near $(\pm\pi/2, \pm\pi/2)$, the so-called “Fermi arc”, on which the d -wave SC gap develops below T_c , and the other incoherent antinodal segments of the FS near $(\pm\pi, 0)$ and $(0, \pm\pi)$, on which a pseudogap (PG) starts to open above T_c .^{32–36} Recently, it was reported that the gap magnitude at the edges of the coherent nodal FS, Δ_{sc} , dominates T_c through BCS (like) relation $2\Delta_{\text{sc}}=4.3k_{\text{B}}T_c$; that is, Δ_{sc} will play a role as the gap maximum Δ_0 .^{37–40}

In light of the effective SC gap Δ_{sc} on the coherent nodal FS, we can speculate the Ni-impurity effect on the SC gap as follows. Ni impurity will predominantly suppress the SC gap on the edges of the coherent nodal FS but in the vicinity of the nodes, as schematically shown in Fig. 6. Such a suppression of the SC gap, meaning the shrinkage of the coherent nodal SC segment on the FS, is consistent with the recent report of the ARPES study on Eu-Bi2201 .¹³ The shrinkage of the nodal SC segment on the FS will bring about a decrease of Δ_{sc} , and consequently suppress T_c . Since the linear slope of the SC dispersion curve around the nodes decreases only slightly in LSCNO (subsections III A and III B), the magnitude of Δ_{sc} linearly depends on the length $L(y)$ of the SC nodal segments on the FS; i.e. $\Delta_{\text{sc}} \propto L(y)$. In LSCNO, $L(y)$ will scale with $\gamma_n(y) - \gamma_0(y)$, $L(y) \propto \gamma_n(y) - \gamma_0(y)$, as discussed in subsections III B. Therefore, taking into account both relations $\Delta_{\text{sc}} \propto L(y)$ and $L(y) \propto \gamma_n(y) - \gamma_0(y)$, T_c is expected to scale with $\gamma_n(y) - \gamma_0(y)$. Actually, this occurred in the present case, as pointed out in subsection III B (Fig. 4).

The y dependence of the SC condensation energy at $T=0$ K, U_0 , can also be explained within the same framework as in the above discussion. According to the BCS

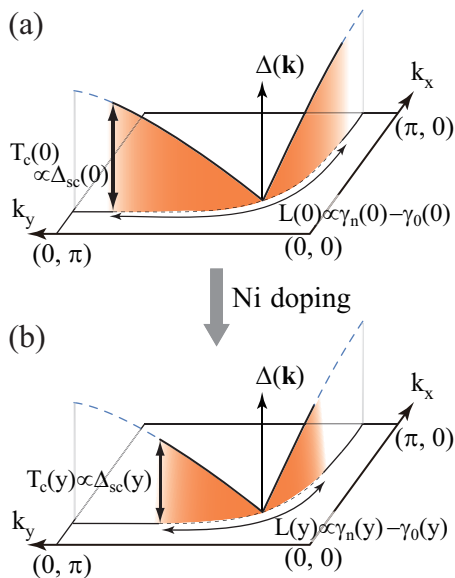


FIG. 6: (Color online) Schematic illustrations of the SC gap in momentum space for pure and Ni-doped LSCO samples.

theory, the SC condensation energy U_0 can be written as follows:

$$U_0 \approx 2.1 \times 10^{-5} \kappa \gamma_n \Delta_0^2 / 2 \quad (4)$$

where prefactor κ is ~ 0.4 for d -wave superconductors, and Δ_0 the d -wave gap amplitude, γ_n the normal state γ value. In LSCNO, $\gamma_n - \gamma_0$ and Δ_{sc} can take the place of γ_n and Δ_0 in Eq. 4 respectively, as mentioned above. In the present study, we estimated the value of $\Delta_{sc}(y)$ from $T_c(y)$ using the BCS relation $2\Delta_{sc} = 4.3k_B T_c$, and calculated U_0 using estimated values of $\Delta_{sc}(y)$ and experimental values of $\gamma_n(y) - \gamma_0(y)$. The calculated values of U_0 are plotted against Ni-concentration y in Fig. 5 for LSCNO with $x=0.14$ and 0.16 . One can see in Fig. 5 that the calculated U_0 values (open symbols) reproduce the experimental ones (closed symbols) of LSCNO well. This finding also supports the present scenario in which the SC gap of LSCNO is locally suppressed around the edge of the coherent nodal FS and the SC gap remains practically intact in the vicinity of the nodes. Such local suppression of the SC gap on the FS will lead to uniform pair breaking in real space, as observed in LSCNO.

IV. SUMMARY

In this study, to elucidate the Ni-impurity effect on the SC gap of high- T_c cuprates, we investigated the H dependence and T dependence of the electronic specific heat in $\text{La}_{2-x}\text{Sr}_x\text{Cu}_{1-y}\text{Ni}_y\text{O}_4$ (LSCNO). The obtained results can be summarized as follows.

1. The residual γ value of LSCNO at $T=0$ K, γ_0 , increases with the application of H along the direction perpendicular to the CuO_2 plane. The increase of γ_0 , $\Delta\gamma_0$, follows the Volovik relation $\Delta\gamma_0 = A\sqrt{H}$, characteristic of d -wave superconductivity with line nodes, indicating that definite nodes remain in the SC gap in LSCNO.

2. In LSCNO, the SC part of C_{el}/T , $\gamma_s \equiv C_{el}/T - \gamma_0$, exhibits a SC anomaly with an abrupt increase at T_c and T -linear dependence at $T \ll T_c$, although $\gamma_0(y)$ is largely enhanced. The T -linear dependence at $T \ll T_c$, characteristic of the existence of the line nodes in the SC gap, is consistent with the results of the magnetic field experiment. Furthermore, it was found for LSCNO that $T_c(y)$ scales with the factor $\gamma_n(y) - \gamma_0(y)$. Such results can be explained by a simple model in which Ni impurities suppress the SC gap predominantly at the edges of the coherent nodal FS, leaving the SC gap virtually unchanged in the vicinity of the nodes.

3. The reduction of U_0 in LSCNO is smaller than the theoretical result for impurities in the unitarity limit, which can explain the reduction of U_0 for Zn impurity very well. In LSCNO, the result of U_0 can be explained as well as T_c within the framework of the present scenario.

Acknowledgments

We are grateful to S. Oinuma, I. Kawasaki and H. Amitsuka for useful experimental support in the specific heat measurements under magnetic fields. We also thank F. J. Ohkawa for valuable discussions. This work was supported in part by a Grant-in-Aid for Scientific Research and the 21st century COE program ‘‘Topological Science and Technology’’ from the Ministry of Education, Culture, Sports, and Technology of Japan.

¹ A. A. Abrikosov and L. R. Gor’kov, Sov. Phys. JETP **12**, 1243 (1961).

² P. W. Anderson, Phys. Rev. Lett. **3**, 325 (1959).

³ J. M. Tarascon, L. H. Greene, P. Barboux, W. R. McKinon, G. W. Hull, T. P. Orlando, K. A. Delin, S. Foner, and E. J. McNiff, Jr., Phys. Rev. B **36**, 8393 (1987).

⁴ G. Xiao, M. Z. Cieplak, J. Q. Xiao, and C. L. Chien, Phys. Rev. B **42**, 8752 (1990).

⁵ Y. Koike, A. Kobayashi, T. Kawaguchi, M. Kato, T. Noji, Y. Ono, T. Hikita, and Y. Saito, Solid State Commun. **82**, 889 (1992).

⁶ K. Ishida, Y. Kitaoka, K. Yamazoe, K. Asayama, and Y. Yamada, Phys. Rev. Lett. **76**, 531 (1996).

⁷ T. Nakano, N. Momono, T. Nagata, M. Oda, and M. Ido, Phys. Rev. B **58**, 5831 (1998).

⁸ T. Adachi, N. Oki, Risdiana, S. Yairi, Y. Koike, and

- I. Watanabe, Phys. Rev. B **78**, 134515 (2008).
- ⁹ B. Nachumi, A. Keren, K. Kojima, M. Larkin, G. M. Luke, J. Merrin, O. Tchernyshov, Y. J. Uemura, N. Ichikawa, M. Goto, and S. Uchida, Phys. Rev. Lett. **77**, 5421 (1996).
- ¹⁰ H. Hiraka, D. Matsumura, Y. Nishihata, J. Mizuki, and K. Yamada, Phys. Rev. Lett. **102**, 037002 (2009).
- ¹¹ S. Haas, A. V. Balatsky, M. Sigrist, and T. M. Rice, Phys. Rev. B **56**, 5108 (1997).
- ¹² T. Kurosawa, N. Momono, H. Amitsuka, M. Oda, and M. Ido, Physica C **470**, S42 (2010).
- ¹³ Y. Okada, T. Kawaguchi, M. Ohkawa, K. Ishizaka, T. Takeuchi, S. Shin, and H. Ikuta, Phys. Rev. B **83**, 104502 (2011).
- ¹⁴ T. Sato, K. Terashima, K. Nakayama, S. Souma, T. Takahashi, T. Yamamoto, and K. Kadowaki, Phys. Rev. B **78**, 100502(R) (2008).
- ¹⁵ G. E. Volovik, JETP Lett. **58**, 469 (1993).
- ¹⁶ K. A. Moler, D. J. Baar, J. S. Urbach, R. Liang, W. N. Hardy, and A. Kapitulnik, Phys. Rev. Lett. **73**, 2744 (1994).
- ¹⁷ M. Nohara, H. Suzuki, M. Isshiki, N. Mangkorkong, F. Sakai, and H. Takagi, J. Phys. Soc. Jpn. **69**, 1602 (2000).
- ¹⁸ H.-H. Wen, L. Shan, X.-G. Wen, Y. Wang, H. Gao, Z.-Y. Liu, F. Zhou, J. Xiong, and W. Ti, Phys. Rev. B **72**, 134507 (2005).
- ¹⁹ T. Nagata, N. Momono, S. Takahashi, M. Oda, and M. Ido, Physica C **264-365**, 353 (2001).
- ²⁰ N. Momono, T. Matsuzaki, M. Oda, and M. Ido, J. Phys. Soc. Jpn. **71**, 2832 (2002).
- ²¹ T. Matsuzaki, N. Momono, M. Oda, and M. Ido, J. Phys. Soc. Jpn. **73**, 2232 (2004).
- ²² N. Momono, M. Ido, T. Nakano, M. Oda, Y. Okajima, and K. Yamaya Physica C **233**, 395 (1994).
- ²³ N. Momono and M. Ido, Physica C **264**, 311 (1996).
- ²⁴ For a review on the low energy quasiparticles, see N. E. Hussey Adv. Phys. **51**, 1685 (2002).
- ²⁵ R. Gilardi, J. Mesot, A. Drew, U. Divakar, S. L. Lee, E. M. Forgan, O. Zaharko, K. Conder, V. K. Aswal, C. D. Dewhurst, R. Cubitt, N. Momono, and M. Oda, Phys. Rev. Lett. **88**, 217003 (2002).
- ²⁶ K. Terashima, H. Matsui, T. Sato, T. Takahashi, M. Kofu, and K. Hirota, Phys. Rev. Lett. **99**, 017003 (2007).
- ²⁷ M. Shi, J. Chang, S. Pailhes, M. R. Norman, J. C. Campuzano, M. Mansson, T. Claesson, O. Tjernberg, A. Bendounan, L. Patthey, N. Momono, M. Oda, M. Ido, C. Mudry, and J. Mesot, Phys. Rev. Lett. **101**, 047002 (2008).
- ²⁸ T. Yoshida, X. J. Zhou, D. H. Lu, S. Komiya, Y. Ando, H. Eisaki, T. Kakeshita, S. Uchida, Z. Hussain, Z.-X. Shen, and A. Fujimori, J. Phys.: Condens. Matter **19**, 125209 (2007).
- ²⁹ J. W. Loram, K. A. Mirza, J. R. Cooper, W. Y. Liang, and J. M. Wade, J. Supercond. **7**, 243 (1994).
- ³⁰ Y. Sun and K. Maki, Phys. Rev. B **51**, 6059 (1995).
- ³¹ T. Toyama and F. J. Ohkawa, J. Phys. Soc. Jpn. **78**, 094712 (2009).
- ³² M. R. Norman, H. Ding, M. Randeria, J. C. Campuzano, T. Yokoya, T. Takeuchi, T. Takahashi, T. Mochiku, K. Kadowaki, P. Guptassarma, and D. G. Hinks, Nature (London) **392**, 157 (1998).
- ³³ M. Le Tacon, A. Sacuto, A. Georges, G. Kotliar, Y. Gallaris, D. Colson, and A. Forget, Nature Phys. **2**, 537 (2006).
- ³⁴ W. S. Lee, I. M. Vishink, K. Tanaka, D. H. Lu, T. Sasagawa, N. Nagaosa, T. P. Devereaux, Z. Hussain, and Z.-X. Shen, Nature (London) **450**, 81 (2007).
- ³⁵ T. Kondo, R. Khasanov, T. Takeuchi, J. Schmalian, and A. Kaminski, Nature (London) **457**, 296 (2009).
- ³⁶ Y. H. Liu, Y. Toda, K. Shimatake, N. Momono, M. Oda, and M. Ido, Phys. Rev. Lett. **101**, 137003 (2008).
- ³⁷ T. Yoshida, M. Hashimoto, S. Ideta, A. Fujimori, K. Tanaka, N. Mannella, Z. Hussain, Z.-X. Shen, M. Kubota, K. Ono, S. Komiya, Y. Ando, H. Eisaki, and S. Uchida, Phys. Rev. Lett. **103**, 037004 (2009).
- ³⁸ T. Kurosawa, T. Yoneyama, Y. Takano, M. Hagiwara, R. Inoue, N. Hagiwara, K. Kurusu, K. Takeyama, N. Momono, M. Oda, and M. Ido, Phys. Rev. B **81**, 094519 (2010).
- ³⁹ M. Ido, N. Momono, and M. Oda, J. Low Temp. Phys. **117**, 329 (1999).
- ⁴⁰ M. Oda, R. M. Distasupil, N. Momono, and M. Ido, J. Phys. Soc. Jpn. **69**, 983 (2000).